3-1-1992

Vibrational Branching Ratios From The Dissociation Of The NeIBr Van Der Waals Molecule

Sarah Anne Walter , '91

Thomas Alex Stephenson
Swarthmore College, tstephe1@swarthmore.edu

Vibrational branching ratios from the dissociation of the NeIBr van der Waals molecule

Sarah A. Walter and Thomas A. Stephenson

Citation: The Journal of Chemical Physics **96**, 3536 (1992); doi: 10.1063/1.461908
View online: http://dx.doi.org/10.1063/1.461908
View Table of Contents: http://scitation.aip.org/content/aip/journal/jcp/96/5?ver=pdfcov
Published by the AIP Publishing

Vibrational branching ratios from the dissociation of the NeIBr van der Waals molecule

Sarah A. Walter and Thomas A. Stephenson[a)]
Department of Chemistry, Swarthmore College, Swarthmore, Pennsylvania 19081

(Received 30 August 1991; accepted 21 November 1991)

The degree of vibrational excitation in the IBr fragment from the vibrational predissociation of NeIBr ($A\ ^3\Pi_1$) has been measured using two-color pump–probe laser-induced fluorescence spectroscopy. We find that for the lowest initial vibrational states examined, $\Delta v = -1$ dissociation pathways dominate the dynamics, while this channel is closed for $v \geqslant 17$. From this result, the A state binding energy (D_0) of the complex is determined to be $67 \pm 4\ cm^{-1}$, while that in the X electronic state is found to be $73 \pm 4\ cm^{-1}$. The X state binding energy is identical to that for NeI_2 and $NeBr_2$, suggesting that the potential energy surface for NeIBr can be constructed from a summation of atom–atom pair potentials; we present such a model potential energy surface. The variations in the vibrational branching ratios, when combined with the trends in the predissociation rates, point to the importance of fragment rotational excitation in the dynamics of the dissociation.

I. INTRODUCTION

A fundamental goal of modern experimental research in physical chemistry and chemical physics has been a detailed understanding of atom–diatom interaction potentials and the dynamics that they support. The study of rare gas–halogen van der Waals molecules has occupied a central position in this field. For example, the dissociation dynamics of a variety of rare gas–I_2 complexes were examined by Levy and co-workers using both laser-induced fluorescence excitation spectra and dispersed emission studies.[1] These experiments focused on measurement of the structures and vibrational predissociation lifetimes of the complexes, as well as the I_2 quantum state distributions that resulted from their dissociation. The spectral resolution afforded by wavelength resolved emission restricted these latter studies to determination of the I_2 vibrational state populations, however. An additional complication in such experiments is that dispersed emission studies of species entrained in the directed mass flow of a supersonic free jet expansion are limited to those with relatively short excited state lifetimes, as longer lived molecules are swept out of the field of view of the monochromator entrance slit prior to emitting. For the diatomic halogens and interhalogens, these restrictions are particularly severe. As a result, dispersed emission spectroscopy has been applied to only I_2- and Br_2-containing complexes excited to the $B(^3\Pi_{0^+_u})$ electronic state.[1,2]

More recently, a two-color pump–probe technique that overcomes both of these deficiencies has been applied to the measurement of the distribution of rotational states populated in the dissociation of complexes such as NeICl (Refs. 3 and 4) and $NeCl_2$ (Ref. 5) by Lester and co-workers and Janda and co-workers, respectively. In this technique a "pump" laser prepares the complex in a specified vibrational state (and in the case of Cl_2-containing complexes, a specified rotational state) in an excited electronic state. After an appropriate delay, chosen to assure dissociation of the complex, the quantum state distribution of the fragments are interrogated by a "probe" laser, which excites the fragments to a higher electronic state. By scanning the wavelength of the probe laser while holding the pump laser wavelength fixed, a fluorescence excitation spectrum of the nascent photofragments is obtained. We have applied the pump–probe technique to an examination of the IBr quantum state distribution that results from dissociation of the NeIBr van der Waals molecule. While our ultimate goal is to measure both the rotational and vibrational state distributions, we focus in this report on the vibrational branching ratios.

In an earlier publication, we have described our examination of the $A\ ^3\Pi_1 \leftarrow X\ ^1\Sigma^+$ fluorescence excitation spectrum of the $NeI^{79}Br$ species.[6] We found that all of the features are extensively homogeneously broadened, with an overall width that varied sharply with IBr vibrational level. From these contours and estimates of the underlying inhomogeneous rotational structure, we found that the vibrational predissociation lifetime of NeIBr varies from $\approx$23 ps for $v = 12$ to $\approx$3 ps for $v = 19$. (Throughout this manuscript, we use the quantum number v to refer to the number of quanta in the I–Br stretching vibration in both the complex and the diatomic fragment.) These lifetimes are consistent with the "energy gap" or "momentum gap" laws in that the lifetime of the excited complex decreases with increasing values of v.[7] According to these models, vibrational predissociation of the complex is enhanced when the amount of energy that must be channeled into the relative translation of the fragments (in this case Ne + IBr) is small. If, for example, the complex dissociates with the loss of one quantum of I–Br stretching vibration (a "$\Delta v = -1$ process"), then the amount of energy available to both the relative translation of the fragments and rotational excitation of IBr is simply the gap between the binding energy (D_0) of the complex and the vibrational spacing in IBr. In one particularly simple formulation of this principle, the rotational degree of freedom of the diatomic fragment is ignored and all of the available energy is assumed to be channeled into relative translation.[7]

a) Author to whom all correspondence should be addressed.

 0021-9606/92/053536-06$06.00

As v increases, the spacing between adjacent vibrational energy levels decreases due to anharmonicity. Thus, one expects that complexes with higher initial vibrational quantum numbers will undergo more efficient dissociation, as the energy available for relative translation decreases. The uniform variation in the experimentally determined NeIBr predissociation lifetimes suggests that this simplified model is adequate. This disscussion assumes, however, that $\Delta v = -1$ dissociation processes are energetically accessible for all of the vibrational levels considered in our earlier study. The results of our present investigation demonstrate that this is not the case for NeIBr and that the $\Delta v = -1$ dissociation channel is energetically open for some vibrational levels, but closed for others.

A second assumption in this description of the energy gap model is that the degree of rotational excitation of the diatomic fragment is either insignificant or invariant to the initial vibrational quantum number. The measurement of rotational distributions has proved to be important in our understanding of the similar ICl- (Refs. 3 and 4) and Cl_2- (Ref. 5) containing complexes and is the dominant aspect of the work now underway in our laboratory.

II. EXPERIMENT

The vacuum chamber and signal detection system utilized in this work are the same as those described previously.[6] Briefly, NeIBr complexes are formed when a 3% Ne/97% He gas mixture is passed over room temperature IBr crystals and expanded into a stainless steel vacuum chamber. The expansion source is a pulsed solenoid valve (General Valve) with a 150 μm diam orifice. The total gas resevoir pressure is fixed at 350 psig. The $A \leftarrow X$ fluorescence excitation features of $NeI^{79}Br$ are located by scanning the wavelength of a Nd^{3+}-YAG pumped dye laser (the "pump" laser; Continuum Lasers YG580-30/TDL-50) while detecting total emission intensity with a red-sensitive photomultiplier tube (Thorn/EMI 9816B). Typically, this laser operates with LD700 laser dye (Exciton), producing an energy of ≈ 13 mJ per pulse at 715 nm. For measurement of photofragment vibrational distributions, the pump laser's wavelength is fixed on a NeIBr $A \leftarrow X$ transition, thus specifying the I–Br stretching quantum number in the electronically excited complex. Our probe laser is a N_2-pumped dye laser (Laser Photonics UV24/DL14P) operating without the intercavity étalon with BBQ laser dye (Exciton). The pulse energy of this laser is attenuated using colored glass neutral density filters to $\leqslant 75$ nJ. The 10 ns probe laser pulse is timed to arrive at the interaction region of the supersonic jet expansion 50–100 ns after the pump laser pulse with a digital delay generator (PAR 9650). The probe laser excites nascent, electronically excited IBr photofragments to the β ion-pair electronic state. (At the probe laser pulse energies utilized in this study, we did not observe any effects due to saturation of the intense $\beta \leftarrow A$ electronic transition.) We detect the total $\beta \rightarrow A$ emission intensity with a blue-sensitive photomultiplier tube (Thorn/EMI 9813QB) as a function of probe laser wavelength to record a fluorescence excitation spectrum of the photofragments. The relative intensities of the features in these spectra are related to the relative population of IBr fragments in the A electronic state vibrational manifold. All fluorescence and laser normalization signals are processed by gated integrators (Stanford Research Systems SR250) and transferred to a laboratory computer for data storage and processing.

Extraction of the relative populations in the A state vibrational levels from the integrated intensity of $\beta \leftarrow A$ fluorescence excitation features requires knowledge of the relevant $\beta \leftrightarrow A$ Franck–Condon factors. Using the available spectroscopic constants for the A (Refs. 8 and 9) and β (Ref. 10) electronic states, we have calculated Rydberg–Klein–Rees (RKR) potential energy curves,[11] evaluated the vibrational wave functions and calculated vibrational overlap integrals.[12] The Franck–Condon factors that are relevant to this study are given in Table I. Experimentally, we have tested the adequacy of these calculations by preparing uncomplexed IBr in one of several vibrational levels in the A state with the pump laser, while scanning the probe laser to measure the intensity of the $\beta \leftarrow A$ transitions that originate in a single A state vibrational level. In these experiments, we observed no deviations in the relative ordering of transition intensities as compared to the calculations but did find that the intensity ratios were not always in quantitative agreement with the calculated values. While this experiment is not a direct calibration of our relative detection sensitivity to population in different A state vibrational levels, our results suggest that the calculated Franck–Condon factors are accurate to $\pm 25\%$. This significant deviation is presumably due to the irregular shape of the A state potential energy curve, such that up to 9 terms in an anharmonic expansion are required to fit the observed vibrational energy level spacings.[9]

TABLE I. Calculated $\beta \leftrightarrow A$ Franck–Condon factors for $I^{79}Br$.

	$v_\beta = 0$	1	2	3	4	5
$v_A = 10$	0.123	0.133	0.060	0.005	0.007	0.033
11	0.239	0.074	5×10^{-5}	0.031	0.052	0.029
12	0.299	5×10^{-4}	0.060	0.056	0.008	0.005
13	0.214	0.157	0.047	2×10^{-5}	0.034	0.038
14	0.062	0.329	0.038	0.045	0.027	0.002
15	0.001	0.143	0.347	0.007	0.009	0.051
16	0.003	3×10^{-4}	0.195	0.340	0.005	0.001
17	3×10^{-4}	0.015	0.003	0.186	0.324	0.013
18	3×10^{-4}	1×10^{-4}	0.036	0.036	0.108	0.272

III. RESULTS AND DISCUSSION

We have measured the vibrational branching ratios in the IBr photofragments that result from the dissociation of NeIBr in the $v = 12$–18 vibrational levels in the A electronic state. We are unable to examine the photofragments that result from excitation in the A state with $v < 12$ due to very poor Franck–Condon overlap with the ground electronic state. The extensive homogeneous broadening of the van der Waals features associated with $v > 18$ precludes investigation of NeIBr molecules with this level of vibrational excitation.

In Fig. 1, we show a scan of the fragment fluorescence excitation spectrum that arises following excitation of NeIBr to the $v = 12$ level. Features corresponding to the (0,11) and (0,10) $\beta \leftarrow A$ transitions in IBr are readily apparent, demonstrating the appearance of both $\Delta v = -1$ and -2 dissociation channels. This spectrum is typical of that observed for the lowest vibrational levels examined in this work ($v = 12$–14) in that the $\Delta v = -1$ channel dominates the dynamics, with a relatively minor contribution from the $\Delta v = -2$ process. There is no evidence for dissociation into the $\Delta v = -3$ channel at this level of vibrational excitation. In Table II, we present the experimentally determined branching ratios for all of the vibrational levels examined. In each case, the relative intensity of a given pair of excitation features is determined by digital integration of the peak areas, followed by application of the calculated Franck–Condon factors to convert experimental intensities to relative populations. For each value of v, we have arbitrarily normalized the branching ratios so that the dominant channel is assigned a value of 1.0. Beginning with $v = 15$, the $\Delta v = -3$ channel is observed with detectable intensity, while the $\Delta v = -1$ channel remains open and dominant. At $v = 16$, approximately equal numbers of NeIBr molecules dissociate with the loss of one and two quanta of vibrational excitation. As shown in Fig. 2, at $v = 17$, however, the $\Delta v = -1$ channel effectively disappears. For the highest vibrational levels examined ($v = 17,18$), the $\Delta v = -2$ dissociation pathway dominates the disposal of vibrational energy.

TABLE II. NeIBr vibrational branching ratios and lifetimes.

Initial v	$\Delta v = -1$	$\Delta v = -2$	$\Delta v = -3$	Lifetime (ps)[a]
12	1.0	0.20	···	23 ± 7
13	1.0	0.20	···	20 ± 4
14	1.0	0.24	···	11 ± 2
15	1.0	0.40	0.13	10 ± 1
16	1.0	0.71	0.19	···
17	0.04	1.0	0.32	8.6 ± 0.7
18	<0.02	1.0	0.40	5.9 ± 0.4

[a] Reference 6.

We interpret the sudden loss of the $\Delta v = -1$ dissociation pathway at $v = 17$ as due to reaching the energetic threshold to fragmentation with the loss of only one quanta of I–Br stretching vibration. When we excite NeIBr to an energy level correlating with $v = 16$ in uncomplexed IBr, we do observe $v = 15$ IBr fragments, demonstrating that the dissociation energy D_0 of the complex is smaller than the 69.6 cm^{-1} spacing between the $v = 16$ and $v = 15$ levels in IBr. On the other hand, the absence of $v = 16$ fragments when NeIBr is excited to a level correlating with $v = 17$ IBr indicates that D_0 for the complex is larger than the 63.9 cm^{-1} spacing between $v = 16$ and $v = 17$ in IBr.[13] (The very small contribution from the $\Delta v = -1$ channel at $v = 17$ displayed in Fig. 2 and recorded in Table II may arise from excitation of a small number of NeIBr complexes with sufficient rotational energy to overcome the $\Delta v = -1$ energetic threshold. As noted earlier, the pump laser wavelength has been adjusted to excite the midpoint of a homogeneously broadened $A \leftarrow X$ NeIBr excitation feature. We are, there-

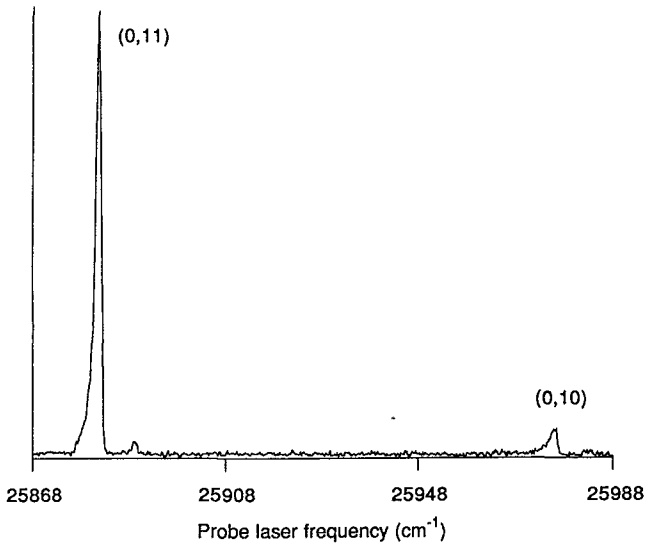

FIG. 1. $\beta \leftarrow A$ fluorescence excitation scan of the A electronic state IBr photofragments produced in the dissociation of NeIBr, $v = 12$. The (0,11) and (0,10) $\beta \leftarrow A$ transitions are identified.

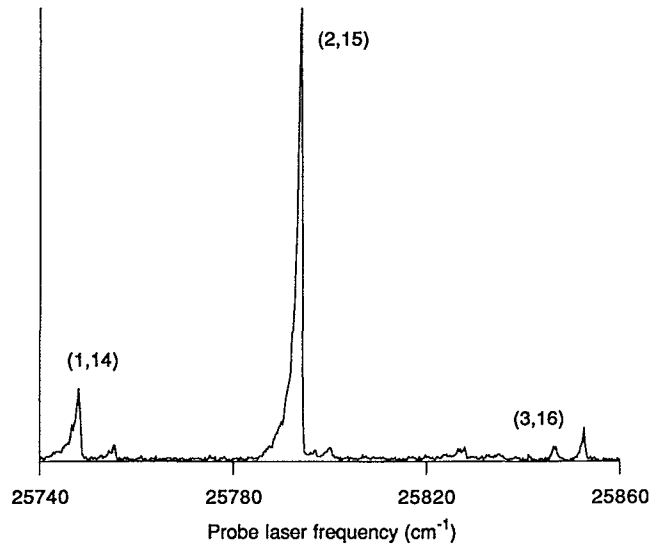

FIG. 2. $\beta \leftarrow A$ fluorescence excitation scan of the A electronic state IBr photofragments produced in the dissociation of NeIBr, $v = 17$. The (3,16), (2,15), and (1,14) $\beta \leftarrow A$ transitions are identified.

fore, unable to control the rotational energy or angular momentum of the initially excited complex.) These results allow us to determine the A state value of D_0 for NeIBr as being 67 ± 4 cm^{-1}. By noting that the shift in the $A \leftarrow X$ excitation frequency between IBr and NeIBr represents the difference in the NeIBr dissociation energies for the X and A electronic states, we can calculate the X state value of D_0. NeIBr excitation features are shifted to the high frequency side of the corresponding IBr transitions by ≈ 6 cm^{-1}, demonstrating that the dissociation energy in the X state exceeds that in the A state by 6 cm^{-1}.[6] We therefore find that D_0 in the X state is 73 ± 4 cm^{-1}.

This value of D_0 should be compared with those for the ground electronic states of NeI_2, 73 ± 2 cm^{-1},[14] and $NeBr_2$, 70 ± 2 cm^{-1}.[2] The close correspondence between all three of these values raises two important points with respect to the construction of potential energy surfaces for rare gas–halogen van der Waals molecules. First, the use of a sum of atom–atom pair potentials to approximate these surfaces would appear to be quantitatively correct in the region near the minimum energy configuration. Such model potentials have formed the basis for numerous simulations of the dynamics of rare gas–halogen complexes.[15] These comparisons are complicated by the fact that the experimentally determined quantities are D_0 values, not the D_e values that would be calculated using a pair potential model for the surface. Because all of these molecules involve a relatively light rare gas atom, Ne, bound to the heaviest diatomic halogens, one might expect, however, similar amounts of zero-point energy in the van der Waals stretching and bending vibrations. Thus, for this series of complexes, one expects that the similarity of the D_0 values is reflective of similar "classical" dissociation energies D_e.

Second, the similarity of the binding energies for a Ne atom with the heteronuclear IBr and the homonuclear I_2 and Br_2 confirms the general premise that the presence of a molecular dipole moment does not significantly impact the strength of the van der Waals interaction. The dominance of the dispersion interaction over the dipole-induced dipole potential is suggested by the description of these interactions for large Ne–IBr distances.[16] The demonstrated adequacy of this assumption at the small (3–5 Å) nuclear separations that characterize the minimum energy configuration of van der Waals molecules further reinforces the general validity of the pair potential approach to triatomic van der Waals systems involving highly polarizable species.

In our earlier report of the $A \leftarrow X$ fluorescence excitation spectrum of NeIBr, we described our attempts to discern the geometry of the complex from the overall symmetry and width of the excitation features.[6] Our conclusion was that the appearance of the excitation features was most consistent with a linear geometry for the complex, though a nonlinear geometry could not be ruled out. The major uncertainty in this analysis was the appropriate rotational temperature for the complex and the adequacy of a Boltzmann distribution to represent the rotational populations. Certain evidence in the excitation spectra, such as the regularity of the band-shifts between IBr, NeIBr, and Ne_2IBr were strongly suggestive of a nonlinear, near T-shaped geometry. The binding energies presented above provide further evidence that the NeIBr complex is nonlinear. Both NeI_2 and $NeBr_2$ have been found to be T-shaped; we find it unlikely that NeIBr would assume a radically different geometry, but would emerge with the same dissociation energy as NeI_2 and $NeBr_2$.

To test these assertions, we have constructed a potential energy surface for NeIBr based on the atom–atom pair potential approach described earlier. We assume that the Ne–IBr interaction potential energy at a particular point in space can be represented as the sum of Ne–I and Ne–Br interactions. The individual atom–atom interactions are modeled as Morse potentials; the potential parameters used in our calculation are displayed in Table III. These parameters were chosen by first beginning with those that describe the Ne–Kr and Ne–Xe van der Waals interaction.[14,17] These data were then used to construct potential energy surfaces for the $NeBr_2$ and NeI_2 van der Waals molecules. The Morse parameters r_{av} and D_e were adjusted from the values appropriate for the rare gas dimers to reproduce the dissociation energies and average bond lengths of NeI_2 (Ref. 14) and $NeBr_2$.[2,18] (The average bond length for NeI_2 has not been determined experimentally. Within experimental error the rare gas–halogen bond length is the same in $HeBr_2$ (Ref. 19) and $NeBr_2$ (Ref. 18) and in $HeCl_2$ (Ref. 20) and $NeCl_2$.[21] We have, therefore, assumed that the NeI_2 bond length will be the same as that for HeI_2.[22]) The range parameters α were maintained at the values provided by the Ne–Kr and Ne–Xe interactions. As in the present study, the experimentally measured binding energies for NeI_2 and $NeBr_2$ are D_0 values, while the potential energy calculations provide values of D_e. Blazy *et al.*, however, have estimated the zero-point energy in NeI_2 to be ≈ 12 cm^{-1}.[14] We adopted this value to our calculation of the NeI_2 dissociation energy and assume a similar value for $NeBr_2$. (We note that the zero-point energy calculation carried out by Blazy *et al.* includes only the van der Waals stretching degree of freedom and no bending vibrations. Their value is, however, consistent with the somewhat higher value, ≈ 17 cm^{-1}, found by Reid *et al.* for $NeCl_2$ in a three-dimensional quantum mechanical bound state calculation.[23] The smaller reduced mass for the Ne–Cl_2 system should introduce a larger measure of zero-point energy.)

We have used these refined Ne–I and Ne–Br potential parameters, without further adjustment, to calculate the potential energy surface for NeIBr. (The I–Br bond length was fixed at its X state equilibrium value of 2.469 Å.[24]) A contour plot of the result is shown in Fig. 3. The minimum energy point on the surface lies at a radial distance of 4.1 Å and at an angle of 70°, as measured from the center of mass of IBr

TABLE III. Atom–atom interaction parameters used in the construction of the NeIBr potential energy surface.

	D_e (cm^{-1})	r_{av} (Å)	α (Å^{-1})
Ne–I	43.0	4.55	1.54
Ne–Br	42.0	3.90	1.67

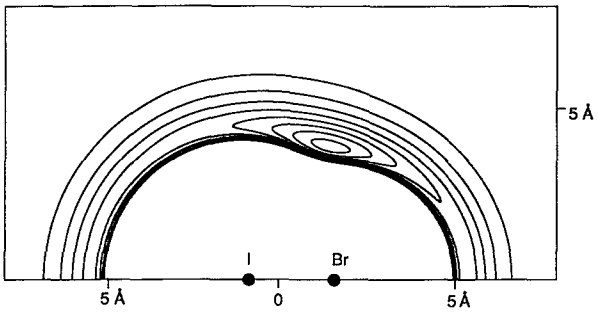

FIG. 3. Model potential energy surface for NeIBr. The origin of the coordinate system is fixed at the center of mass of IBr. The energy contours are drawn at 10 cm^{-1} intervals, with the outermost contour lying -10 cm^{-1} relative to the energy of separated Ne + IBr.

and relative to the I–Br bond. The minimum energy is -85 cm^{-1} relative to the energy of Ne + IBr, a result that is excellent agreement with the experimentally determined D_0 value, in the likely situation that the zero-point energy lies between 8 and 16 cm^{-1}. We thus find that the atom–atom pair potential approach provides a potential energy surface that is consistent with all of the experimental data on the minimum energy configuration for the NeIBr system.

The data reported here, when combined with that presented previously on the vibrational predissociation lifetimes of the NeIBr complex,[6] provide a qualitative test of certain aspects of the "energy gap" or "momentum gap" concepts. Consider the variation, with v, of the predissociation lifetimes of NeIBr (Table II). Over the range $v = 12$–15, we note that as predicted by these models, the lifetime decreases as the amount of energy available to relative translation of the fragments decreases. Based the dissociation energy calculated above, at $v = 15$, there is at most 7 ± 4 cm^{-1} of available translational energy. With the closure of the $\Delta v = -1$ channel, however, there are no longer any energetically open dissociation pathways with such small amounts of energy released to the translational degrees of freedom. If rotational excitation of the diatomic fragment is ignored, one expects an increase in the lifetime (decrease in the rate of vibrational predissociation) at the point that the $\Delta v = -1$ channel closes. Such effects have been observed in both HeI_2 (Ref. 25) and $NeBr_2$.[26] In these cases, there are decreases in the homogeneous linewidths of the relevant excitation features for vibrational levels for which the $\Delta v = -1$ process is inaccessible. We do not observe such an effect in the dissociation of NeIBr. One possible explanation for this result is that as compared to Br_2- and I_2-containing complexes, the rotational degree of freedom in the IBr fragment is unusually active in the dissociation. Such activity would tend to smooth over variations in the dissociation lifetimes, as the rotational degree of freedom is available to absorb the energy released by the dissociation.

This explanation is counter, however, to our classical intuition regarding the conservation of angular momentum, which constrains the amount of energy that can be absorbed by rotation of IBr. Assuming that we initially excite only complexes with total angular momentum of zero, to conserve angular momentum any rotational excitation of IBr must be balanced by a corresponding degree of orbital angular momentum of the recoiling Ne + IBr fragments. (As noted earlier, we are unable to control the J state of the complex that we prepare in the electronically excited A state. Given supersonic free jet conditions, however, it is likely that our sample includes exclusively complexes with limited amounts of total angular momentum.) If we assume that similar amounts of fragment orbital angular momentum appear in the dissociation of, for example, NeIBr and $NeBr_2$, we expect similar amounts of rotational angular momentum in the diatomic fragments. Our basis for this assumption is the model potential energy surface for NeIBr, which suggests that the classical impact parameters for the "half-collision" scattering events in the dissociation of IBr-, Br_2-, and I_2-containing complexes will be approximately the same. Since the rotational constant of IBr is intermediate to that of I_2 and Br_2, the constraint on the amount of energy distributed into rotation of the diatomic fragment should not be radically different.

Our results suggest that this intuitive classical approach is inadequate and that a simplified (i.e., ignoring the rotational degree of freedom) energy gap model fails as well. Perhaps the deviation from a T-shaped geometry that we predict for NeIBr and/or the presence of a molecular dipole moment leads to increased excitation of IBr rotation (and fragment orbital angular momentum). For example, while the dipole-induced dipole attraction between Ne and IBr (calculated using simple electrostatic considerations[16]) is small compared to the dispersion interaction, it is both anisotropic and large compared to the rotational spacing in IBr. In this case, the IBr dipole moment may have a negligible impact on the equilibrium structure and binding energy, but may play a significant role in modulating the photodissociation dynamics. If correct, then this effect should be apparent in the distribution of rotational states populated in IBr by the dissociation, particularly for those vibrational levels in the vicinity of the $\Delta v = -1$ threshold. High resolution scans of the contours observed in spectra such as Figs. 1 and 2 are now underway in our laboratory and should serve to illuminate this behavior.

ACKNOWLEDGMENTS

This research has been supported by grants from the National Science Foundation (Grant No. CHE-8915038), the Research Corporation, and the Swarthmore College Faculty Research Fund. Acknowledgment is made to the Donors of The Petroleum Research Fund, administered by the American Chemical Society, for partial support of this research.

[1] D. H. Levy, Adv. Chem. Phys. **47**, 323 (1981).
[2] J. I. Cline, D. D. Evard, B. P. Reid, N. Sivakumar, F. Thommen, and K. C. Janda, in *Structure and Dynamics of Weakly Bound Molecular Complexes*, edited by Alfons Weber (Reidel, Dordrecht, 1987), pp. 533–551.
[3] J. C. Drobits and M. I. Lester, J. Chem. Phys. **88**, 120 (1987).
[4] J. C. Drobits and M. I. Lester, J. Chem. Phys. **89**, 4716 (1988).
[5] J. I. Cline, N. Sivakumar, D. D. Evard, C. R. Bieler, B. P. Reid, N. Halberstadt, S. R. Hair, and K. C. Janda, J. Chem. Phys. **90**, 2605 (1989).
[6] W. R. Simpson and T. A. Stephenson, J. Chem. Phys. **90**, 3171 (1989).
[7] J. A. Beswick and J. Jortner, Adv. Chem. Phys. **47**, 363 (1981); G. E. Ewing, J. Phys. Chem. **91**, 4662 (1987).
[8] M. Suzuki and T. Fujiwara, J. Mol. Spectrosc. **133**, 233 (1989).

[9] B. Guo and J. Tellinghuisen, J. Mol. Spectrosc. **127**, 222 (1988).
[10] J. C. D. Brand, A. R. Hoy, and A. C. Risbud, J. Mol. Spectrosc. **113**, 47 (1985).
[11] Calculated using the program RKR1 by R. J. LeRoy, 1983; we are grateful to Professor LeRoy for supplying a copy of this program.
[12] R. J. LeRoy, University of Waterloo Chemical Physics Research Report, No. CP-230R3 (1986).
[13] The A state vibrational intervals used in this section are derived from our examination of the $A \leftarrow X$ fluorescence excitation spectrum of jet-cooled IBr. These intervals agree within 0.3 cm^{-1} with those found by L.-E. Selin, Ark. Fys. **21**, 479 (1962).
[14] J. A. Blazy, B. M. DeKoven, T. D. Russell, and D. H. Levy, J. Chem. Phys. **72**, 2439 (1980).
[15] See, for example, J. A. Beswick and J. Jortner, J. Chem. Phys. **68**, 2277 (1978); J. I. Cline, B. P. Reid, D. D. Evard, N. Sivakumar, N. Halberstadt, and K. C. Janda, *ibid.* **89**, 3535 (1988); O. Roncero, J. A. Beswick, N. Halberstadt, P. Villarreal, and G. Delgado-Barrio, *ibid.* **92**, 3348 (1990).
[16] J. O. Hiscshfelder, C. F. Curtis, and R. B. Bird, *Molecular Theory of Gases and Liquids* (Wiley, New York, 1954), pp. 22–30.
[17] J. M. Parson, T. P. Schafer, F. P. Tully, P. E. Siska, Y. C. Wong, and Y. T. Lee, J. Chem. Phys. **53**, 2123 (1970).
[18] F. Thommen, D. D. Evard, and K. C. Janda, J. Chem. Phys. **82**, 5295 (1985).
[19] L. J. van de Burgt, J.-P. Nicolai, and M. C. Heaven, J. Chem. Phys. **81**, 5514 (1984).
[20] J. I. Cline, D. D. Evard, F. Thommen, and K. C. Janda, J. Chem. Phys. **84**, 1165 (1986).
[21] D. D. Evard, F. Thommen, and K. C. Janda, J. Chem. Phys. **84**, 3630 (1986).
[22] R. E. Smalley, L. Wharton, and D. H. Levy, J. Chem. Phys. **68**, 671 (1978).
[23] B. P. Reid, K. C. Janda, and N. Halberstadt, J. Phys. Chem. **92**, 587 (1988).
[24] K. P. Huber and G. Herzberg, *Molecular Spectra and Molecular Structure IV* (van Nostrand, New York, 1979), p. 338.
[25] W. Sharfin, P. Kroger, and S. C. Wallace, Chem. Phys. Lett. **85**, 81 (1982).
[26] B. A. Swartz, D. E. Brinza, C. M. Western, and K. C. Janda, J. Phys. Chem. **88**, 6272 (1984).